JOURNAL OF MATERIALS SCIENCE 35 (2000) 1359–1364

Degradation of an alkyd polymer coating characterized by AC impedance

JAY J. SENKEVICH*
Department of Chemical and Metallurgical Engineering, University of Nevada, Reno, NV 89557, USA
E-mail: senkej@rpi.edu

Alternating current (AC) impedance was used to evaluate the degradation of a high solids alkyd primer paint coating in a 3% NaCl solution, a 100% relative humidity (RH) environment after immersion in a 3% NaCl solution, and a 95% RH environment after immersion in a 3% NaCl solution. The results indicate AC impedance measures the amount of water absorbed into the coating through resistance results. A significant increase in capacitance may indicate a build up of corrosion products which causes blistering or debonding at the coating/metal interface, which may also be determined by diffusion tail analysis.

1. Introduction

Electrochemical impedance spectroscopy (EIS) has been extensively used to study paint coating systems [1–14]. In contrast to EIS, alternating current (AC) impedance is a dry method. In, EIS an alternating potential is applied to an immersed specimen and the current response is measured. AC impedance, used in this study, applies an alternating potential across a specimen in ambient air after previous immersion or atmospheric exposure and measures the current response. The resulting impedance, which is the ratio of the applied potential to the current response, possesses components of resistance, capacitance, and sometimes mass transport (Warburg impedance).

AC impedance does not require immersion and is therefore suitable for the in situ testing of paints and coatings in the atmosphere or in other actual service environments. Direct measurement in situ of coating degradation makes AC impedance a potentially powerful technique, because a coating could be replaced before extensive surface damage of the underlying metal occurs. AC impedance may elucidate the coating degradation processes making degradation prediction easier. The work here explores the coating degradation process by use of resistance, capacitance, and diffusion tail analysis obtained from AC impedance.

2. Background

Bacon *et al.* [15] investigated the degradation of polymer coatings by measuring their DC resistance. Wormwell and Brasher [16] followed by Brasher and Kingsbury [17], introduced the single frequency capacitance method to evaluate water uptake of polymer coated metals previously immersed in sea water. The results of these two capacitance studies were compared to the classical weight gain gravimetric method to evaluate coating degradation but discrepancies existed. Touhasent and Leidheiser [18] correlated the long-term performance of a coated metal with its initial increase in capacitance. These studies gave the first indications that electrical methods provided an abundance of information about polymer coating degradation. A series of papers in 1976 described the electrical response of polymer coatings as a function of frequency [19–21]. Impedance analysis by use of the Nyquist complex plane and Bode plots were used to analyze the data. More recent work involving EIS by Mansfeld and Kendig related water uptake to the capacitance of polymer coatings [22].

Earlier work by Wei *et al.* [23] showed the effects of different chloride concentrations on the same high solids alkyd primer coating used in this study. Tap water, low in chloride, took much longer to degrade the coatings than the 3% NaCl solution. In this previous study, 3 days of exposure to tap water gave a resistance of 1 Mohm while exposure to 3% NaCl solution gave a resistance of 0.5 Mohm for the same time. The difference became more pronounced as the exposure time increased. A correlation apparently exists between chloride concentration and the rate of coating degradation. As opposed to EIS, AC impedance does not possess solution resistance because it is a dry method, but it does possess the analogous contact resistance. Except for the conceptual difference between contact and solution resistance AC impedance and EIS model the same in terms of equivalent circuits.

The most fundamental circuit for a mass/charge transfer system is the Randles equivalent circuit (Fig. 1). The Randles Circuit, in terms of this investigation, describes the response of a single-step charge transfer process with diffusion of reactants, products,

* *Present Address*: Department of Physics SC 1C25, Rensselaer Polytechnic Institute, 110 Eighth St., Troy NY 12180.

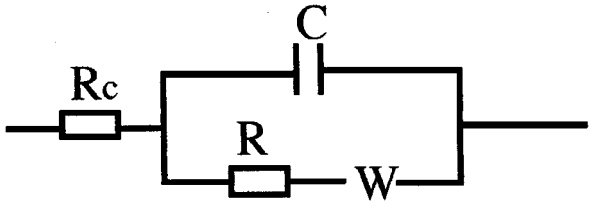

Figure 1 Randles circuit for a polymer coated metal system possessing charge and mass transfer processes.

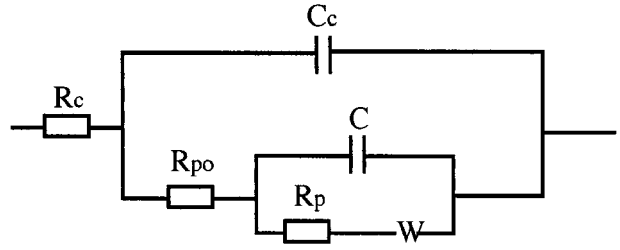

Figure 2 An equivalent circuit taking into consideration the corrosion at the metal/coating interface and for the charge transport through the coating, in addition to the mass transport through the coating.

or both, to or from the coating metal interface and diffusion within the coating itself. The Warburg impedance W is given by [24]:

$$W = \sigma\omega^{-1/2}(1-j)\tanh\left\{\delta\left(\frac{j\omega}{D}\right)^{1/2}\right\} \quad (1)$$

where σ is the Warburg coefficient, analogous to the mass transfer coefficient, and δ is the Nernst diffusion layer thickness, which is also the thickness of the hypothetical stagnant diffusion layer. D is the diffusion coefficient of the electroactive species, w is the angular frequency, and $j^2 = -1$. Calculating the magnitude of the impedance for the Randles circuit in terms of the basic circuit elements gives:

$$Z(j\omega) = R_c + \frac{R+W}{1+j\omega C(R+W)} \quad (2)$$

where R is the resistance coating metal system, C is the capacitance of the coating metal system which includes the capacitance of the coating and the coating/metal interface, W is the Warburg impedance, and R_c is the contact resistance between the electrode and the coating. Separating Equation 2 into its real and imaginary components gives:

$$Z_{\text{real}} = \frac{(R+W)+R_c+\omega^2C^2(R+W)^2R_c}{1+\omega^2C^2(R+W)^2} \quad (3)$$

$$Z_{\text{imag}} = \frac{-\omega C(R+W)^2}{1+\omega^2C^2(R+W)^2} \quad (4)$$

As the frequency decreases the Warburg impedance dominates because of the $\omega^{-1/2}$ term in Equation 1.

More complex equivalent circuits exist (Fig. 2) which take into consideration the different kinds of capacitance's and resistance's which are present in a coating undergoing degradation [25, 26]. C_c is the coating's capacitance, which depends on its dielectric constant ε and its thickness L.

$$C_c = \frac{\varepsilon\varepsilon_o A}{L} \quad (5)$$

Mansfeld and Kendig named R_{po} the pore resistance or more generally the coating resistance, attributing it to the formation of ionically conducting pathways in the coating [22, 25, 26]. R_p is the charge transfer resistance created at the metal/coating interface and C is the corresponding capacitance at that interface. R_c is the contact resistance analogous to the solution resistance discussed previously. Solving the equivalent circuit for the complex impedance gives:

$$Z(jw) = R_c + \frac{R_{po}+(R_p+W)+j\omega CR_{po}(R_p+W)}{1-\omega^2CC_cR_{po}(R_p+W)+j\omega[(C+C_c)(R_p+W)+R_{po}C_c]} \quad (6)$$

For the present study, the more basic Randles circuit was used to constrain the system to three parameters, namely capacitance, resistance and Warburg impedance. This is because $\tau_{max} = R_pC$ (at the interface) for this study is possibly superimposed on the diffusion tail and only $\tau_{max} = R_cC_c$ (in the coating) is well defined. Therefore, due to this lack of differentiation modeling is not sensitive to each separate capacitance and resistance and as a result large errors would occur.

3. Experimental

Sample panels 305 mm × 100 mm obtained from Advanced Coating Technologies Inc., Hillsdale, Michigan were sheared into 645 mm^2 (1.0 in^2) coupons. The high solids alkyd primer coating, 30 μm thick, had a low resistance to degradation by constant immersion compared to other related primer coatings [23]. Significant degradation resulted after constant immersion of less than one week in 3% NaCl solution. The coupons were degreased by light shaking in a sealed container with a mild detergent (Manostat Aquet, New York, New York) for one minute, rinsed in de-ionized water and air dried. 14 prepared coupons were placed in a covered 3% NaCl solution and 2 coupons were removed every 24 hours for 7 days. Each coupon was patted dry, clamped between two copper electrodes and connected to the impedance analyzer.

Copper multi-strand wire was soldered to 10 mm × 10 mm × 50 μm thick copper foil pads. These electrodes were clamped on both sides of a one-side coated metal sample. The clamp was hand tightened until the electrodes made firm contact with the polymer coating without damaging it. A minimum tightness of the clamp was needed to ensure reproducible results. Fig. 3

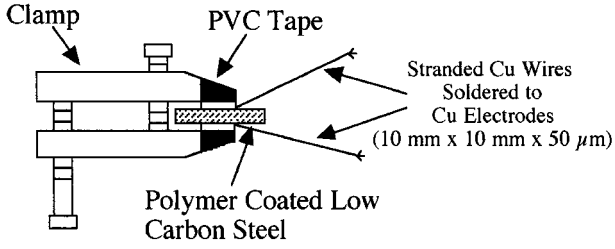

Figure 3 Apparatus used for impedance measurements.

shows the clamping apparatus used in conjunction with the copper electrode leads. PVC electrical tape was wrapped around the clamp faces contacting the copper electrodes. This prevented the existence of parallel currents due to PVC's high resistance. The electrodes in Fig. 3 were connected to a Schlumberger Model SI 1260 Impedance Analyzer with Z60 software (Schlumberger Instruments, Billerica, Massachusetts) and analyzed from 0.1 Hz to 1 MHz with an alternating potential of 60 mV.

Two other experiments tested coating degradation after immersion in a 3% NaCl solution. After 4 days of constant immersion, 10 coupons were placed in a 3×10^{-3} m^3 volume cylindrical closed chamber with a relative humidity of 100%, achieved by adding deionized water at the bottom of the chamber. The ambient temperature varied from 20°C to 28°C. 2 coupons were removed every 24 hours for 4 days and analyzed by AC impedance by the same method as the constant immersion samples.

The third experiment was conducted by using a humidity cabinet made by ESPEC, Grand Rapids, Michigan, model LHU-112. A fan circulated air through the cabinet at $95 \pm 1\%$ relative humidity and at a temperature of 20 ± 1°C. After 4 days of constant immersion 10 coupons were placed in the humidity cabinet. 2 coupons were removed every 4 hours for 24 hours and analyzed by AC impedance by the same method as the constant immersion samples. The resistance R was found by choosing two points from the high frequency end of the Nyquist complex plane plot. The computer, using those two points, created a data set composed of all the data points between the two points and drew a semicircle by an arc fit method. The highest point on the semicircle derived from the Nyquist complex plane plot gave f_{max} used to calculate the capacitance.

4. Results

4.1. Resistance of the coating

Figs 4–6 show Nyquist complex plane plots for the degradation of the alkyd primer coating after constant immersion in 3% NaCl solution at successively longer times. Measurements could not be obtained before two days of constant immersion because the coating resistance exceeded the measurement capability of the impedance analyzer (30 MΩ). Up till two days of constant immersion water apparently had not been absorbed into the coating. After two days of constant immersion no diffusion tail is present indicating a lack of diffusion of the electroactive species, in this case the chloride ion. After three days of constant immersion the diffusion tail is present. Diffusion tails are also present in Figs 7 and 8 for the coatings exposed to 3% NaCl solution for 4 days of constant immersion and then the samples were taken out and placed in a

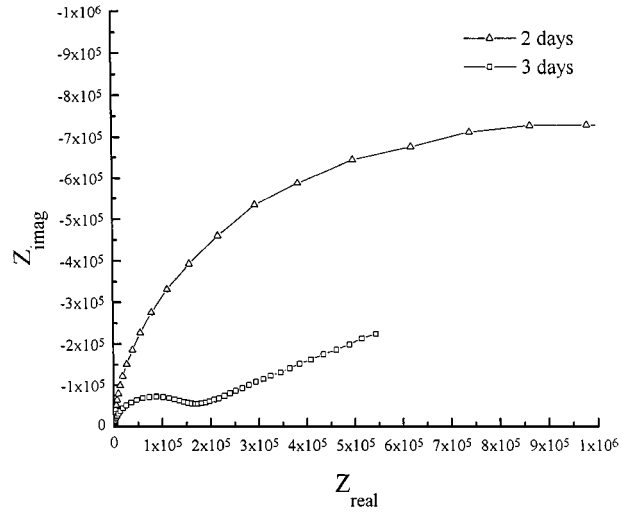

Figure 4 Nyquist complex plane plot for the alkyd coating exposed to constant immersion in 3% NaCl solution for 2 and 3 days.

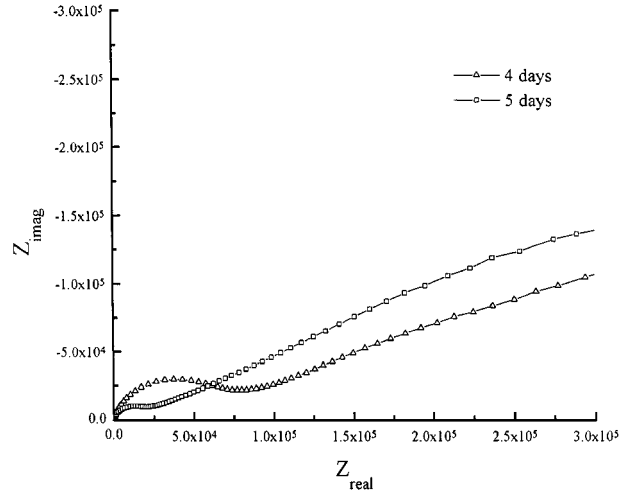

Figure 5 Nyquist complex plane plot for the alkyd coating exposed to constant immersion in 3% NaCl solution for 4 and 5 days.

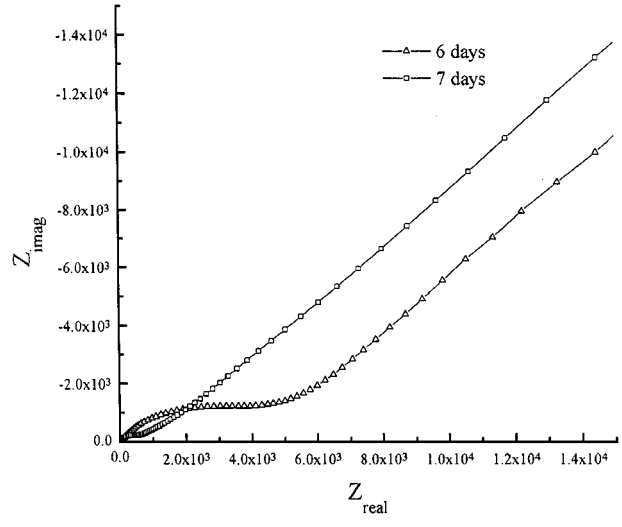

Figure 6 Nyquist complex plane plot for the alkyd coating exposed to constant immersion in 3% NaCl solution for 6 and 7 days.

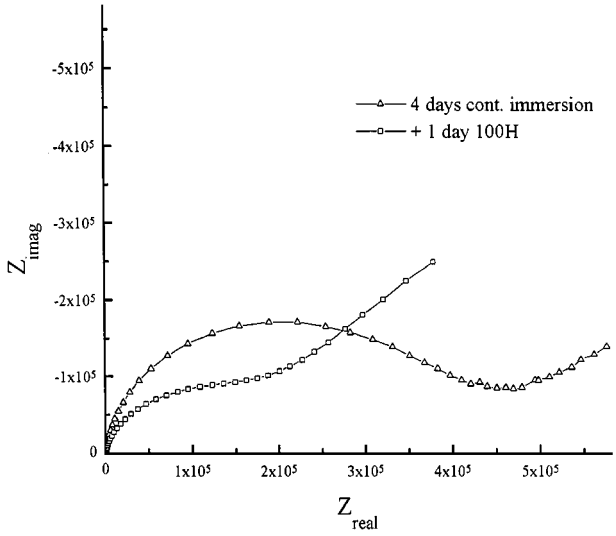

Figure 7 Nyquist complex plane plot for the alkyd coating exposed to constant immersion for 4 days then exposed to a 100% RH free convection environment for 1 day.

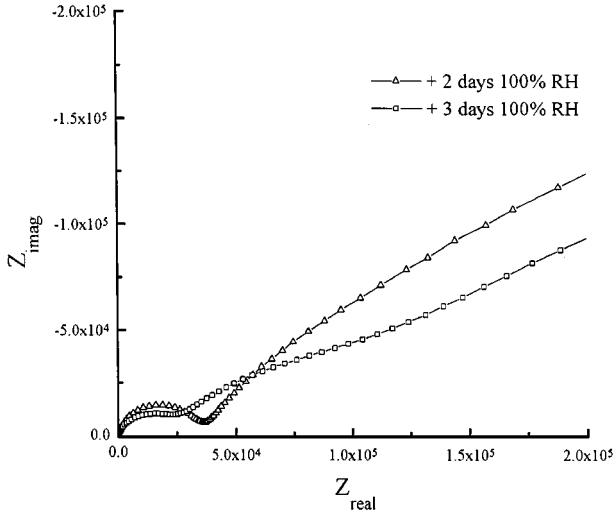

Figure 8 Nyquist complex plane plot for the alkyd coating exposed to constant immersion for 4 days then exposed to a 100% RH free convection environment for 2 and 3 days.

humidity chamber at 100% relative humidity. Analysis of the diffusion tails will be discussed later.

Fig. 9 shows the logarithm of the coating resistance versus exposure time. The error bars represent 95% confidence intervals. All three experiments are represented in the figure: constant immersion in 3% NaCl, 4 days of constant immersion in 3% NaCl followed by 100% relative humidity free convection environment, and 4 days of constant immersion in 3% NaCl followed by 95% relative humidity forced convection environment. The logarithmic decrease in coating resistance is typical for the incorporation of water into a polymer coating [28]. The coating's resistance for constant immersion decreased 0.59 log decades/day whereas the 100% RH coating decreased 0.37 log decades/day. The difference is attributable to the 100% RH environment being less severe than constant immersion. After placement of the coating into the 100% RH environment no additional chloride ions become incorporated into the film, thus the driving force for degradation is less. However, degradation continues to occur due to the chloride already present in the film from the constant immersion. At 4 days exposure, all the data points should have the same resistance. The constant immersion coating has a lower resistance at 4 days of exposure due to use of a different alkyd coated panel. This maybe the same reason for the rather large variability in the 100% RH data.

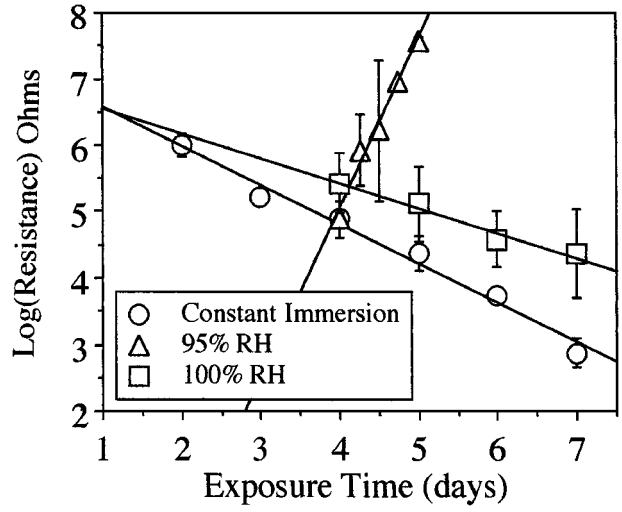

Figure 9 Log(Resistance) versus exposure time in days for the alkyd coating exposed to constant immersion, constant immersion then 100% RH, and constant immersion then 95% RH.

The coating placed in the 95% RH environment dried-out due to lack of moisture saturation in the chamber. Its resistance increased 2.55 log decades/day. Visually, the surface of these coatings were dry in marked contrast to the constant immersion and 100% RH coatings. Quite possibly no further coating degradation can take place without the presence of water and a saturated or wet environment. This may mean that chloride can only be "activated" and contribute to coating degradation when ample water is available, which is typical for a corrosion process.

4.2. Capacitance of the coating

The values for the coating capacitance were computed by using:

$$C = \frac{1}{(2\pi f_{\max} R)} \tag{6}$$

which assumes the system can be modeled using a RC circuit with a relaxation time $\tau_{\max} = RC$. Fig. 10 shows the coating capacitance versus exposure time in days for all three experiments. The error bars represent 95% confidence intervals. The constant immersion coating shows a large increase in capacitance due to water incorporation into the coating; and according to Feliu *et al.* [26] "the capacitance only increases substantially when corrosion products accumulate." Corrosion products may include ferric and ferrous hydroxides (FeOOH, $Fe(OH)_2$) and ferric and ferrous chlorides ($FeCl_3$, $FeCl_3 \cdot 6H_2O$, $FeCl_2$, $FeCl_2 \cdot 2H_2O$, $FeCl_2 \cdot 4H_2O$). Accumulation would probably be at the metal/coating interface due to the reaction of chloride with iron. This increase in capacitance is not seen until the fourth day

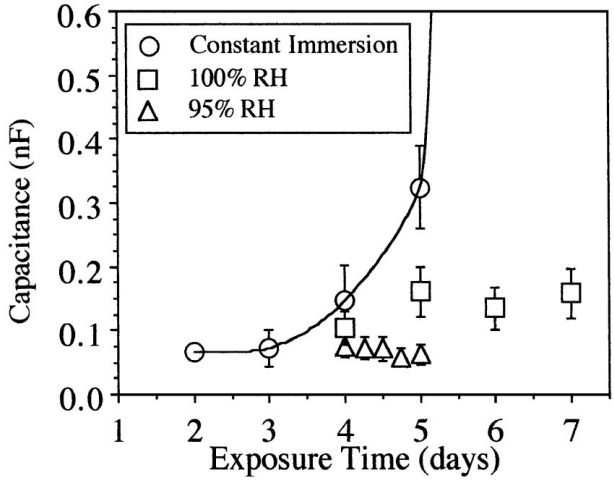

Figure 10 Capacitance versus exposure time in days for the alkyd coating exposed to constant immersion, constant immersion then 100% RH, and constant immersion then 95% RH.

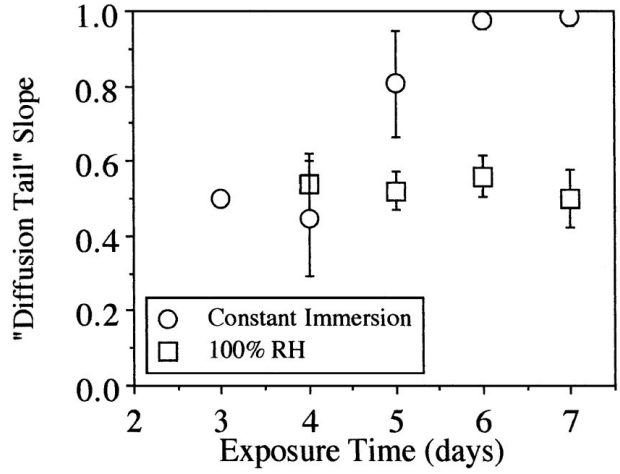

Figure 11 The slope of the apparent diffusion tail (Warburg Impedance) versus exposure time to a constant immersion and constant immersion followed by 100% RH.

of exposure. At day 6 the capacitance dramatically increased to a value of 12.1 ± 5.1 nF at which point macroscopic debonding or blistering occurred and the diffusion tail had a slope of one (discussed in the next section) for the constant immersion sample. The errors in the measurement of capacitance increased as the constant immersion coatings became more degraded (higher capacitance). The alkyd coatings maybe nonhomogenous owing to this variation.

The coatings exposed to 100% RH exhibited a different capacitance response than the constant immersion samples. The capacitance of the 100% RH coatings increased only slightly. The 100% RH environment prevented moisture loss and retained the aggressive chloride ions within the coating but did not further incorporate any additional chloride ions. Therefore, further water incorporation occurred (from resistance data) but no significant buildup of corrosion products occurred leading to a rapid increase in capacitance. The 95% RH coating did not exhibit an increase in capacitance when it dried out. This might be unexpected since water has a high dielectric constant at 25°C ($\varepsilon_r = 78.54$) [29] but the relaxation time for the charge transfer of chloride possibly increased as the resistance of the film increased due to the lack of water facilitating the charge transport across the polymer coating.

4.3. Diffusion tail analysis

The Nyquist complex plane plots for the constant immersion and 100% RH coatings show Warburg behavior but interestingly the slope of the diffusion tail changes as the coating degrades [26]. Fig. 11 shows the slope of the straight-line diffusion tail (Warburg impedance) versus exposure time. Each diffusion tail slope was determined by a computer generated linear regression line from two chosen points from the beginning of the diffusion tail from the low frequency data. As exposure time increased, the slope of the diffusion tail increased until it reached a maximum of one for the constant immersion coating.

For the case of a one-dimensional diffusion controlled reaction Equation 1 is valid and the slope of the diffusion tail in the Nyquist complex plane plot is one. However, from Fig. 11 this case only occurred with the coatings exposed to constant immersion at day 6. The explanation for Fig. 11 lies in the concept of a diffusion controlled reaction given by Equation 1 and the rate of charge transport across the coating given by the relaxation time $\tau_{max} = R_c C_c$, where R_c is the coating resistance and C_c is the coating capacitance; and the rate of reaction at the metal/coating interface given by: $\tau_{max} = R_p C$, where R_p is the charge transfer resistance and C is the capacitance due to the reaction at the coating/metal interface produced from the corrosion products. When the coating is completely dry its resistance is nearly infinite and no diffusion can take place (2 days constant immersion). However, once diffusion can take place two relaxation times maybe evident, one for the coating and one for the reaction at the metal/coating interface. In the present case where two relaxation processes exist, one at the metal/coating interface $\tau_{max} = R_p C$ and one for the charge transport through the coating $\tau_{max} = R_c C_c$, two semicircles might be seen in the Nyquist complex plane plot if the time constants are well separated. However, if diffusion effects are evident then the semicircle which has the longer relaxation will have a diffusion tail superimposed over it. This leads to an apparent diffusion tail which curves toward the real axis. This behavior is evident in Fig. 5 for the constant immersion coatings.

No attempt is made in this study to separate the two resistances and capacitances which exist in the metal/coating system because the three processes: reaction at the metal/coating interface, charge transport through the coating and diffusion of chloride through the coating are not well separated in terms of their time constants. At 7 days of exposure for the constant immersion coating, no obvious semicircle exists and the diffusion tail is the only distinguishing feature of the Nyquist complex plane plot. However, after debonding occurs at day 6 a semicircle is apparent. This semicircle is probably due to the charge transport through the coating, which has the shorter relaxation time compared to the reaction at the metal/coating interface. The reason for this is that when the coating debonds the reaction

rate at that interface is orders of magnitude larger than with a tightly bounded coating. This is mostly due to the tightly constrained corrosion products preventing further corrosion of the metal, effectively acting as a barrier layer. With the presence of debonding or blistering, the process is diffusion limited and the slope of the diffusion tail is one with no bending. Therefore, two indications exist for determining the point at which macroscopic debonding occurs. First, the capacitance increases dramatically and second the diffusion tail has a slope of one with no bending. The 100% RH coating, in contrast, does not show an increase in capacitance due to the tightly bound coating slowing the rate of reaction at the metal/coating interface thus protecting the metal substrate.

5. Conclusions

Constant immersion showed a logarithmic decrease in coating resistance providing evidence for coating degradation due to water incorporation. The substantial increase in capacitance was attributed to the buildup of corrosion products after which point macroscopic debonding occurred. A substantial increase in capacitance maybe due to the significant buildup of corrosion products at the coating/metal interface due to the reaction of chloride with iron. The rate of reaction at the coating/metal interface was slow due to the well-bonded coating but the rate of this reaction increased when debonding occurred. This was due to the corrosion products becoming solvated and diffusing away from the surface, which resulted in diffusion tails with a slope of one due to a diffusion limited transport process.

Resistance continued to decrease during exposure to 100% RH after prior constant immersion. Water and chloride ions retained in the coating from constant immersion continued to attack the coating. However, degradation was less severe due to the dilution of the chloride originally present. Capacitance could not substantially increase because corrosion products could not accumulate. In 95% RH with forced convection, moisture evaporated from the coating increasing the resistance but the lack of water apparently had no effect on the observed capacitance.

Acknowledgements

The author would like to thank Professors Indira Chatterjee and Denny Jones of the University of Nevada, Reno.

References

1. H. XIAO and F. MANSFELD, *J. Electrochem. Soc.* **141** (1994) 2332.
2. A. S. M. RAUTENBACH, P. C. PISTORIUS and J. E. LEITCH, *Poly. Mater. Sci. Eng.* **74** (1996) 14.
3. A. AMIRUDIN and D. THIERRY, *Prog. Org. Coat.* **26** (1995) 1.
4. F. MANSFELD, *Corrosion* **52** (1996) 417.
5. C. COMPÈRE, É. FRECHETTE and E. GHALI, *Corrosion Sci.* **34** (1993) 1259.
6. C-T CHEN and B. S. SKERRY, *Corrosion* **47** (1991) 598.
7. N. PEBERE, T. PICAUD, M. DUPRAT and F. DABOSI, *Corrosion Sci.* **29** (1989) 1073.
8. R. D. ARMSTRONG and D. WRIGHT, *Electrochimica Acta* **38** (1993) 1799.
9. F. DEFLOIAN, L. FEDRIZZI, A. LOCASPI and P. L. BONORA, *Electrochimica Acta* **38** (1993) 1945.
10. R. HIRAYAMA and S. HARUYAMA, *Corrosion* **47** (1991) 952.
11. T. C. SIMPSON, P. J. MORAN, H. HAMPEL, G. D. DAVIS, B. A. SHAW, C. O. ARAH, T. L. FRITZ and K. ZANKEL, *Corrosion* **46** (1990) 331.
12. J. TITZ, G. H. WAGNER, H. SPÄHN, M. EBERT, K. JÜTTNER and W. J. LORENZ, *Corrosion* **46** (1990) 221.
13. S. A. MCCLUNEY, S. N. POPOVA, B. N. POPOV, R. E. WHITE and R. B. GRIFFIN, *J. Electrochem. Soc.* **139** (1992) 1556.
14. J. N. MURRAY and H. P. HACK, *Corrosion* **47** (1991) 480.
15. R. C. BACON, J. J. SMITH and F. M. RUGG, *Ind. Eng. Chem.* **40** (1948) 161.
16. F. WORMWELL and D. M. BRASHER, *Industrie Chim. Belge.* **19** (1954) 813.
17. D. M. BRASHER and A. H. KINGSBURY, *J. Appl Chem.* **4** (1954) 62.
18. R. E. TOUHSAENT and H. LEIDHEISER, *Corrosion* **28** (1972) 435.
19. L. BEAUNIER, I. EPEIBOIN, J. C. LESTRADE and H. TAKENOUTI, *Surf. Tech.* **4** (1976) 237.
20. M. KENDIG and H. LEIDHEISER, *J. Electrochem Soc.* **123** (1976) 982.
21. H. LEIDHEISER and M. KENDIG, *Corrosion* **32** (1976) 69.
22. F. MANSFELD, M. KENDIG and S. TSAI, *Corrosion* **38** (1982) 478.
23. D. F. WEI, I. CHATTERJEE and D. A. JONES, *Corrosion* **51** (1995) 97.
24. S. FELIU JR., R. BARAJAS, J. M. BASTIDAS, M. MORCILLO and S. FELIU, "Electrochemical Impedance: Analysis and Interpretation," edited by J. R. Scully *et al.*, ASTM special technical publication #1188, (Philadelphia, PA, 1993) p. 438.
25. F. MANSFELD, M. KENDIG and S. TSAI, *Corrosion Sci.* **23** (1983) 317.
26. F. MANSFELD and M. KENDIG, "Laboratory Corrosion Tests and Standards," edited by G. S. Haynes and R. Baboian, ASTM special technical publication #866, (Philadelphia, PA, 1985) p. 122.
27. Z60 Inpedance/Gain-Phase Analysis Software Operating Manual, Scribner Assoc. ver 1.3 (1991).
28. E. K. TAN, F. BELLUCCI, M. J. KLOPPERS and R. M. LATANISION, *Mat. Sci. Forum* **111–112** (1992) 177.
29. "Handbook of Chemistry and Physics," edited by C. D. HODGMAN, R. C. WEAST and S. M. SHELBY, 41st ed. (Chemical Rubber Pub. Co., Cleveland, OH, 1959–60) p. 2525.

Received 7 May
and accepted 9 September 1999